

X-entanglement of PDC photon pairs

E. Brambilla, L. Caspani, O. Jedrkiewicz, L. A. Lugiato and A. Gatti*
*INFN-CNR-CNISM, Dipartimento di Fisica e Matematica,
 Università dell'Insubria, Via Valleggio 11, 22100 Como, Italy*

We investigate the spatio-temporal structure of the bi-photon entanglement in parametric down-conversion (PDC) and we demonstrate its non-factorable X-shaped geometry. Such a structure gives access to the ultra-broad bandwidth of PDC, and can be exploited to achieve a bi-photon temporal localization in the femtosecond range. This extreme localization is connected to our ability to resolve the photon positions in the source near-field. The non factorability opens the possibility of tailoring the temporal entanglement by acting on the spatial degrees of freedom of twin photons.

PACS numbers: 42.50.-p,42.50.Ar,42.50.Dv

Parametric down-conversion (PDC) is probably the most efficient and widely used source of entangled photon pairs, which has been employed in several successful implementations of quantum communication and information schemes. At the very heart of such technologies lies the quantum interference between photonic wave functions, which depends crucially on the spatio-temporal mode structure of the photons. In this work, the issue of controlling and tailoring the bi-photon spatio-temporal structure is addressed from a peculiar and novel point of view, that is, the non factorability in space and time of the PDC bi-photon entanglement. The idea comes from the context of nonlinear optics, where recent studies [1] outlined how in nonlinear media the angular dispersion relations impose a hyperbolic geometry involving both temporal and spatial degrees of freedom in a non-factorable way. The wave object that captures such a geometry is the so-called X-wave (the X being formed by the asymptotes of the hyperbola), which is a localized and propagation-invariant wave-packet, non separable in space and time. The statistical counterpart of the X-wave was recently showed to emerge in the X-shaped structure of the classical first order coherence function [2].

In this work, we turn our attention to the genuine quantum properties of PDC, and we adopt the X-wave picture for investigating the spatio-temporal structure of the two-photon entangled state. With few exceptions [3, 4], investigations on the quantum state of PDC have been performed to date mostly either in a purely temporal [5, 6, 7] or spatial [8, 9, 10] framework. Our approach, based on the non-factorability in space and time of the state, will point out relevant elements of novelty, as the possibility of tailoring the temporal bandwidth of the bi-photons by manipulating their spatial degrees of freedom. In particular, by resolving their near-field positions, we will show that the X-structure opens the access to an ultra-broad bandwidth entangled photonic source, with a temporal localization in the femtosecond range. Such an extreme localization can be applied to increase the sensitivity of high precision measurements in the time domain (e.g. in the protocol of clock synchronization [11] or of quantum optical coherence tomography [12]). Our re-

sults compare with recent findings reported in [13], where a $\sim 7fs$ Hong-Ou-Mandel dip was observed through the use of a quasi-phase-matched nonlinear grating.

We shall focus on type I PDC, in the low-gain regime where single pairs of photons can be detected by coincidence counts. We remark that the X-structure of entanglement is a general feature of PDC, present also in type II and in the high-gain regime [14].

The model is basically the same as in [4, 10]. A quasi-monochromatic and coherent pump field propagates along the direction z inside a slab of nonlinear $\chi^{(2)}$ crystal of length l_c . $\hat{A}_p(\vec{x}, t, z)$, $\hat{A}_s(\vec{x}, t, z)$ denote the envelope operators of the pump and the down converted signal field, of central frequencies ω_p and $\omega_s = \omega_p/2$, respectively. Here $\vec{x} = (x, y)$ labels the transverse coordinates, while t is time. We next pass to the Fourier domain: $\hat{A}_i(\vec{q}, \omega, z) = \int \frac{d^2\vec{q}}{2\pi} \int \frac{d\omega}{\sqrt{2\pi}} \hat{A}_i(\vec{x}, t, z) e^{-i\vec{q}\cdot\vec{x} + i\omega t}$, $i = s, p$ and extract the fast variation due to their linear propagation along the crystal slab:

$$\hat{A}_i(\vec{q}, \omega, z) = e^{ik_{iz}(\vec{q}, \omega)z} \hat{a}_i(\vec{q}, \omega, z) \quad i = s, p, \quad (1)$$

where $k_{iz}(\vec{q}, \omega) = \sqrt{k_i^2(\vec{q}, \omega) - \omega^2}$ is the z -component of the wave vector of the i -th field, $k_i(\vec{q}, \omega)$ being the wave number at frequency ω , which for the extraordinary wave depends also on the propagation direction, identified by the transverse wave-vector \vec{q} . The fields \hat{a}_i defined in this way have a slow variation along the crystal, arising only from the nonlinear interaction. In the low-gain regime we can assume that the pump is undepleted by the nonlinear interaction, so that $\frac{d}{dz} \hat{a}_p(\vec{q}, \omega, z) = 0$, and substitute its field operator by a c -number field $\alpha_p(\vec{q}, \omega)$. In this way, the pump evolution along the crystal is described by $\mathcal{A}_p(\vec{q}, \omega, z) = e^{ik_{pz}(\vec{q}, \omega)z} \alpha_p(\vec{q}, \omega)$. For the down-converted signal field, its propagation along the crystal is described by the equation [4]:

$$\frac{\partial \hat{a}_s(\vec{q}, \omega, z)}{\partial z} = \frac{g}{l_c} \int \frac{d^2\vec{q}'}{2\pi} \int \frac{d\omega'}{\sqrt{2\pi}} [\alpha_p(\vec{q} + \vec{q}', \omega + \omega') \times \hat{a}_s^\dagger(\vec{q}', \omega', z) e^{-i\Delta(\vec{q}, \omega, \vec{q}', \omega')z}] , \quad (2)$$

where g is the dimensionless parametric gain, proportional to the second-order $\chi^{(2)}$ susceptibility, to the crys-

tal length l_c and to the pump peak value (the pump field has been normalized to its peak value). The phase-mismatch function

$$\Delta(\vec{q}, \omega, \vec{q}', \omega') = k_{sz}(\vec{q}, \omega) + k_{sz}(\vec{q}', \omega') - k_{pz}(\vec{q} + \vec{q}', \omega + \omega') \quad (3)$$

determines how efficiently a pump photon with transverse wave-vector $\vec{q} + \vec{q}'$ and frequency $\omega_p + \omega + \omega'$ is down-converted into a pair of photons with transverse wave-vectors \vec{q}, \vec{q}' and frequencies $\omega_s + \omega, \omega_s + \omega'$: the smaller its modulus, the higher the probability that such an elementary process occurs.

In most experiments in the low gain regime, the quantity of primary interest is the two-photon correlation, also called *bi-photon amplitude*. We shall study this quantity in the spatio-temporal domain, in a plane at the output face of the crystal (*near-field region*), that is, we focus on

$$\psi(\vec{x}, t, \vec{x}', t') = \langle \hat{A}_s(\vec{x}, t, l_c) \hat{A}_s(\vec{x}', t', l_c) \rangle. \quad (4)$$

In the low gain limit considered in this work its square modulus $|\psi(\vec{x}, t, \vec{x}', t')|^2$ is proportional to the two-photon coincidence rate $G^{(2)}(\vec{x}, t, \vec{x}', t')$, which gives the joint probability distribution of finding two photons in position \vec{x} at time t and position \vec{x}' at time t' , respectively.

For small gains ($g \ll 1$), the propagation equation (2) can be solved perturbatively up to first order in g , obtaining the following expression for the bi-photon amplitude in the Fourier domain:

$$\begin{aligned} \langle \hat{A}_s(\vec{q}_1, \omega_1, l_c) \hat{A}_s(\vec{q}_2, \omega_2, l_c) \rangle &= g \mathcal{A}_p(\vec{q}_1 + \vec{q}_2, \omega_1 + \omega_2, l_c) \\ &\times (2\pi)^{-3/2} e^{i \frac{\Delta(\vec{q}_1, \omega_1, \vec{q}_2, \omega_2) l_c}{2}} \text{sinc} \left[\frac{\Delta(\vec{q}_1, \omega_1, \vec{q}_2, \omega_2) l_c}{2} \right] \end{aligned} \quad (5)$$

In the literature the same quantity is usually derived through a perturbative evaluation of the two-photon state vector (see e.g. [3]).

In order to simplify our results, we consider the limit of a nearly plane-wave and monochromatic pump, i.e, a pump of duration τ_p and waist w_p large enough, so that the dependence of the phase-mismatch Δ on $\vec{q}_1 + \vec{q}_2$ and $\omega_1 + \omega_2$ (the pump variables) can be neglected. It can be shown [14] that such an approximation holds when w_p and τ_p are much larger than the spatial walk-off and the temporal delay due to group velocity mismatch, respectively, experienced by the signal and the pump after crossing the crystal. Typical values are $\sim 300 \mu\text{m}$ and $\sim 2\text{ps}$, as in the example of a 4 mm β -barium-borate (BBO) crystal cut for degenerate type I PDC at 352 nm. Provided that we are in such conditions, the bi-photon amplitude (4) at the crystal output face takes the factorized form:

$$\psi(\vec{x}, t, \vec{x}', t') = \mathcal{A}_p \left(\frac{\vec{x} + \vec{x}'}{2}, \frac{t + t'}{2}, l_c \right) \psi_{\text{pw}}(\vec{x} - \vec{x}', t - t') \quad (6)$$

where

$$\psi_{\text{pw}}(\vec{x}, t) = \int \frac{d^2 \vec{q}}{(2\pi)^2} \int \frac{d\omega}{2\pi} e^{i\vec{q} \cdot \vec{x} - i\omega t} V(\vec{q}, \omega) \quad (7a)$$

$$V(\vec{q}, \omega) = g e^{i \frac{\Delta_{\text{pw}}(\vec{q}, \omega) l_c}{2}} \text{sinc} \left[\frac{\Delta_{\text{pw}}(\vec{q}, \omega) l_c}{2} \right], \quad (7b)$$

$$\Delta_{\text{pw}}(\vec{q}, \omega) = k_{sz}(\vec{q}, \omega) + k_{sz}(-\vec{q}, -\omega) - k_p(0, 0) \quad (7c)$$

is the PWP result for the field correlation function. The pump beam profile $\mathcal{A}_p(\vec{x}, t, l_c)$ acts thus as a slow modulation over the PWP correlation $\psi_{\text{pw}}(\vec{x}, t)$, as it can be expected in the nearly stationary and homogeneous conditions considered here.

A first qualitative insight into the problem can be obtained by considering the usual quadratic expansion of the phase matching function, equivalent to adopting the paraxial and quadratic dispersion approximations. In the case of e-oo phase matching, it takes the form [4]:

$$\Delta_{\text{pw}}(\vec{q}, \omega) l_c \approx \Delta_0 + \frac{\omega^2}{\Omega_0^2} - \frac{q^2}{q_0^2}, \quad (8)$$

where $\Delta_0 = (2k_s - k_p)l_c$ is the collinear phase mismatch at degeneracy, $\Omega_0 = \sqrt{1/k_s'' l_c}$, $q_0 = \sqrt{k_s/l_c}$, and we used the short-hand notation $k_s = k_s(0, 0)$, $k_p = k_p(0, 0)$, $k_s'' = d^2 k_s / d\omega^2|_{0,0}$. If we extend the validity of such an approximation to the entire (\vec{q}, ω) domain, and we use the identity $e^{ip/2} \text{sinc}(p/2) = \int_0^1 ds e^{isp}$, the bi-photon amplitude $\psi_{\text{pw}}(\vec{x}, t)$ can be recasted in the integral form:

$$\psi_{\text{pw}}(r, t) = g \frac{q_0^2 \Omega_0}{8\sqrt{\pi^3 i}} \int_0^1 \frac{ds}{s^{3/2}} e^{\frac{i}{4s}(q_0^2 r^2 - \Omega_0^2 t^2)} e^{is\Delta_0}. \quad (9)$$

where r indicates the radial coordinate. This expression clearly evidences the hyperbolic geometry of $\psi_{\text{pw}}(r, t)$: the function is indeed constant on the rotational hyperboloids where the argument

$$H(r, t) \equiv q_0^2 r^2 - \Omega_0^2 t^2 \quad (10)$$

assumes constant values. However, it can be easily shown that $\psi_{\text{pw}}(H)$ goes as $1/\sqrt{|H|}$ for $|H| \rightarrow 0$, that is, when approaching the asymptotes of the X-structure, where $H(r, t) = q_0^2 r^2 - \Omega_0^2 t^2 = 0$. This singularity arises from the unphysical assumption that the approximation (8) is valid everywhere.

In order to obtain quantitative results we need therefore to drop the approximation (8), and to go beyond the paraxial and quadratic dispersion approximations in the evaluation of $\Delta(\vec{q}, \omega)$. $\psi_{\text{pw}}(\vec{x}, t)$, defined by Eq.(7), is hence numerically calculated by using the complete Sellmeier relations [15] for the refractive indexes. An example of our results is shown by Fig.1 for the case of a type I BBO crystal. Since the signal is an ordinary wave, the spatial radial symmetry of the problem can be exploited to compute Eq.(7) by means of a Fourier-Hankel transform. Correspondingly, the bi-photon amplitude ψ_{pw} depends only on the radial coordinate $r = |\vec{x}|$. A cut of this

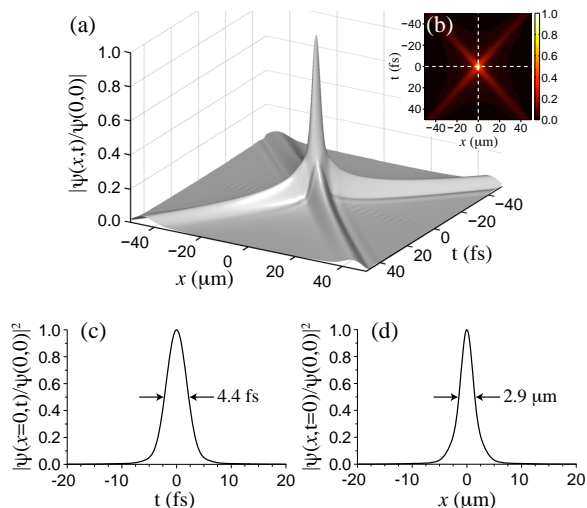


FIG. 1: (Color online)(a) and (b): Modulus of the bi-photon amplitude in the plane (x, t) , clearly displaying its X-shaped geometry (the whole 3-D plot has a rotational symmetry in space). (c) and (d): Cuts of the coincidence rate $|\psi_{pw}(\vec{x}, t)|^2$ along the temporal (c) and the transverse coordinate axis (d) [indicated by the two dashed lines in frame (b)]. The width of the peaks shows the relative temporal and spatial localization of bi-photons. BBO crystal, cut at 33.436° for type I PDC; $g = 10^{-3}$, $\lambda_p = 352\text{nm}$, and $l_c = 4\text{mm}$.

quantity in the (x, t) plane is displayed by frames (a) and (b) of Fig.1 (the whole 3-dimensional plot have a radial symmetry in the space domain, and has therefore a biconical geometry). A clear X-shaped structure emerges: this non-trivial shape of the spatio-temporal two-photon correlation, that we shall call *X-entanglement* can be considered the counterpart, at the level of quantum noise, of the nonlinear X-waves [1]. Similar results hold for a variety of phase-matching conditions, corresponding to different crystal orientations, and for a wide range of crystal lengths [14].

A remarkable characteristic of the X-entanglement is the unusually small width of the spatio-temporal correlation peak, which corresponds to a strong relative localization of twin photons both in time and space. The two lower frames of Fig.1 plot cuts of the two-photon coincidence rate $|\psi_{pw}(\vec{x}, t)|^2$ along the temporal and spatial axis, respectively. The spatial localization is remarkable but not impressive, as displayed by the spatial profile $|\psi_{pw}(x, 0)|^2$ in Fig.1(d), which has a FWHM of $\sim 2.9 \mu\text{m}$. More impressive, and in a sense, unexpected, is the temporal relative localization of twin photons, which can be appreciated from the temporal profile $|\psi_{pw}(0, t)|^2$ in Fig.1(c), which is as narrow as 4.4 fs. Such an ultra-short two-photon localization emerges spontaneously from a nearly monochromatic pump, as a consequence of the ultra-broad bandwidth of PDC phase-matching, which in principle extends over the optical frequency $\omega_p \sim 5 \cdot 10^{15}$ Hz. Notice that, in order to account for e.g. the finite

bandwidth of detection, in our calculations we include a super-gaussian frequency filter centered at degeneracy. The 4.4 fs width of the temporal peak is in practice determined by the width of this frequency filter, (see Fig.2 for a comparative view of the frequency bandwidths involved).

It is interesting to compare our results with the typ-

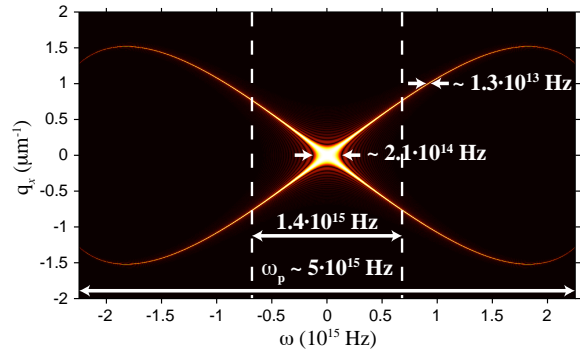


FIG. 2: (Color online) Plot of $|V(q_x, \omega)|$, showing the phase matching curve. The dashed vertical lines show the frequency bandwidth selected by the filter and the arrows indicate the different bandwidths involved (same parameters as in Fig.1).

ical ~ 100 fs temporal localization of the coincidence rate measured in the far-field zone, by collecting twin photons that propagate at symmetric directions \vec{q} and $-\vec{q}$, within a small angular bandwidth. In that case, the measured quantity is proportional to $|V(\vec{q}, t)|^2 = |\int \frac{d\omega}{2\pi} e^{-i\omega t} V(\vec{q}, \omega)|^2$. Its temporal width is determined by the inverse of the bandwidth of the spectrum $V(\vec{q}, \omega)$ at fixed q , i.e. the narrow ($10^{13} - 10^{14}$ Hz) thickness of the curve in Fig.2. This bandwidth can be roughly evaluated as Ω_0 for $q/q_0 \ll 1$, and as $\Omega_0 q_0/q$ for $q/q_0 > 1$. Clearly, since Ω_0 scales as $l_c^{-1/2}$, the shorter the crystal, the stronger the temporal localization in the far-field; however, a far-field localization in the femtosecond range would require a crystal as short as $\sim 50 \mu\text{m}$, with a strongly reduced down-conversion efficiency. Conversely, in our case, the detection of coincidences in the near-field gives in principle access to the full ($\sim 10^{15}$ Hz) bandwidth of phase matching even for a long crystal.

It is however important to stress that such an extreme temporal localization of twin photons relies on the ability to resolve their positions in the near-field plane. Indeed, a measurement collecting all the photons over the beam cross-section, without discriminating their positions, is characterized by the integrated coincidence rate $\int d^2\vec{x} |\psi_{pw}(\vec{x}, t)|^2$, reproduced by the dashed curve in Fig.3, which has a width of $\sim 100\text{fs}$. This may appear surprising, because in this measurement all the photons at the different frequencies within the phase-matching are collected. However, the identity $\int d^2\vec{x} |\psi_{pw}(\vec{x}, t)|^2 = \int d^2\vec{q} |V(\vec{q}, t)|^2$, shows that in this case the coincidence rate takes the form of an *incoherent superposition* of the

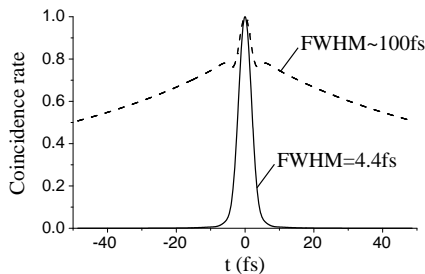


FIG. 3: Solid line: $|\psi_{\text{pw}}(\vec{x}=0, t)|^2$, coincidence rate when photon positions are resolved in the near field. Dashed line: $\int d^2\vec{x} |\psi_{\text{pw}}(\vec{x}, t)|^2$, coincidence rate measured without resolving photon positions

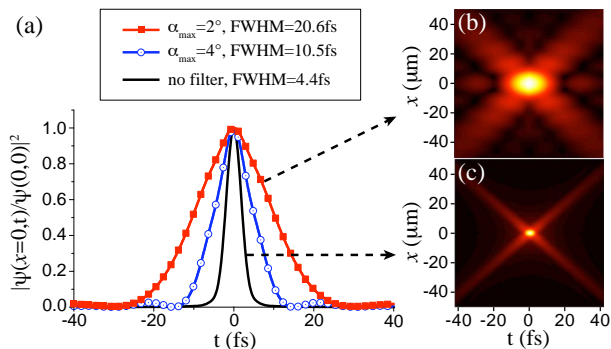


FIG. 4: (Color online) Effect of spatial filtering on the X-entanglement: (a) Temporal correlation peak $|\psi_{\text{pw}}(0, t)|^2$ in the presence of a spatial filter, that cuts the angular spectrum at an angle α_{max} . The two insets show the full X-correlation for $\alpha_{\text{max}} = 2^\circ$ (b), and in the absence of any filter (c).

probabilities of detecting a pair of photons at a given q and has therefore the same $\sim 100\text{fs}$ temporal localization as the far-field coincidence rate at fixed q . Conversely, by resolving the near-field positions of twin photons, the measured quantity is $|\psi_{\text{pw}}(0, t)|^2 = |\int \frac{d^2\vec{q}}{(2\pi)^2} V(\vec{q}, t)|^2$, which corresponds to a *coherent superposition* of the probability amplitudes at a given q (i.e. at a given frequency due to the angle-frequency relation imposed by phase matching), and therefore allows a stronger temporal localization.

The non-factorability in space and time of the X-entanglement thus opens the relevant possibility of tailoring the temporal bandwidth of the bi-photons by acting on their spatial degrees of freedom. As a more specific example, let us consider the effects of spatial filtering on the temporal correlation. Let us assume that a $4f$ lens system is employed to image the near-field of the PDC fluorescence, and that a circular aperture of radius r_a is located in the far-field $2f$ plane, acting as a filter that cuts all the angular spectrum at $\alpha > \alpha_{\text{max}} = \arcsin(r_a/f)$. Fig. 4 shows the effect of such a spatial filter on the temporal correlation peak. While in the absence of any spatial filter the correlation shows a strong temporal lo-

calization, as the angular bandwidth is reduced by spatial filtering, the two-photon correlation broadens in time. This is a clear effect of the non-factorability of the correlation, because, thanks to the shape of the angular spectrum shown in Fig.2, a spatial filter that cuts the angular bandwidth has also the effect of cutting the frequency bandwidth.

In conclusions, this work demonstrates the hyperbolic geometry underlying the two-photon PDC entanglement and its non-factorability with respect to space and time. As for the X-waves encountered in nonlinear optics, the X-shape of the bi-photon correlation is imposed by the phase-matching mechanism governing the PDC process, and following this analogy we coined the name of X-entanglement. The key element of novelty brought by this structure is its extreme localization, with correlation times and correlation lengths in the femtosecond and micrometer range, respectively. The strong temporal localization is determined by the full extent of the PDC bandwidth, rather than by the bandwidth $\sim \Omega_0$ characterizing the PDC far-field. For this reason, a near field measurement scheme able to resolve spatially the coincidences would provide a powerful tool for high-precision measurements, capable of improving substantially the resolution power in the temporal domain with respect to standard schemes. Furthermore, we have shown how the non-factorability of the structure gives the possibility of tailoring the temporal entanglement through manipulations of the spatial degrees of freedom.

We thank P.Di Trapani and M. Clerici for useful discussions. We acknowledge the financial support of the FET programme of the EC, under the GA HIDEAS FP7-ICT-221906.

* Corresponding author: A. Gatti:alessandra.gatti@mi.infn.it

- [1] For a review see C. Conti and S. Trillo in *Localized Waves*, p. 243, H.E. Hernandez-Figueroa, M. Zamboni-Rached and E. Recami eds. (Wiley-Interscience, 2007).
- [2] O. Jedrkiewicz, A. Picozzi, M. Clerici, D. Faccio, and P. Di Trapani, Phys. Rev. Lett. **97**, 243903 (2006); Phys. Rev. A **76**, 033823 (2007).
- [3] M. Atatüre *et. al.*, Phys. Rev. A **65**, 023808 (2002).
- [4] A. Gatti, R. Zambrini, M. San Miguel, L.A. Lugiato, Phys. Rev. A **68**, 053807 (2003).
- [5] C.K. Hong, Z.Y. Ou, L. Mandel, Phys. Rev. Lett. **59**, 2044 (1987).
- [6] C.K. Law, I.A. Walmsley, and J.H. Eberly, Phys. Rev. Lett. **84**, 5304 (2000).
- [7] W. P. Grice, A. B. U'Ren, and I. A. Walmsley, Phys. Rev. A **64**, 063815 (2001)
- [8] M.H. Rubin, Phys. Rev. A **54**, 5349 (1996)
- [9] C.K. Law and J.H. Eberly, Phys. Rev. Lett. **92**, 127903 (2004).
- [10] A. Gatti, E. Brambilla, L. Lugiato, in Progress in Optics **51**, 251, E.Wolf ed. (2008, Elsevier B.V); E. Brambilla,

- A. Gatti, M. Bache and L.A. Lugiato, Phys. Rev. A **69**, 023802 (2004).
- [11] V. Giovannetti, S. Lloyd, L. Maccone, and F.N.C. Wong, Phys. Rev. Lett. **87** 117902, (2001).
- [12] A. F. Abouraddy, M.B. Nasr, B.E. Saleh, A.V. Sergienko, and M.C. Teich Phys. Rev. A **65**, 053817 (2002).
- [13] M.B. Nasr *et. al.*, Phys. Rev. Lett. **100**, 183601 (2008).
- [14] L. Caspani, E. Brambilla, L. Lugiato, and A. Gatti, preprint.
- [15] N. Boeuf et al., Optical Engineering, **39**, 1016 (2000).